CHEMISTRY
A EUROPEAN JOURNAL

ChemPubSoc
Europe

DOI: 10.1002/chem.201301411

Encapsulation of Metalloporphyrins in a Self-Assembled Cubic M_8L_6 Cage: A New Molecular Flask for Cobalt–Porphyrin-Catalysed Radical-Type Reactions

Matthias Otte,[a] Petrus F. Kuijpers,[a] Oliver Troeppner,[b] Ivana Ivanović-Burmazović,[b] Joost N. H. Reek,[a] and Bas de Bruin*[a]

Dedicated to Prof. Dr. Roeland J. M. Nolte, in honour of his contributions to the field of supramolecular chemistry

Abstract: The synthesis of a new, cubic M_8L_6 cage is described. This new assembly was characterised by using NMR spectroscopy, DOSY, TGA, MS, and molecular modelling techniques. Interestingly, the enlarged cavity size of this new supramolecular assembly allows the selective encapsulation of tetra(4-pyridyl)metalloporphyrins (M^{II}-(TPyP), M = Zn, Co). The obtained encapsulated cobalt–porphyrin embedded in the cubic zinc–porphyrin assembly is the first example of a catalytically active encapsulated transition-metal complex in a cubic M_8L_6 cage. The substrate accessibility of this system was demonstrated through radical-trapping experiments, and its catalytic activity was demonstrated in two different radical-type transformations. The reactivity of the encapsulated Co^{II}(TPyP) complex is significantly increased compared to free Co^{II}(TPyP) and other cobalt–porphyrin complexes. The reactions catalysed by this system are the first examples of cobalt–porphyrin-catalysed radical-type transformations involving diazo compounds which occur inside a supramolecular cage.

Keywords: cubic cages · homogeneous catalysis · host–guest chemistry · radical chemistry · self-assembly

Introduction

The creation of complex, well-defined 3D structures through self-assembly is an important and fast growing field of modern chemistry, leading to new supramolecular architectures with unprecedented functionality.[1] Elegant examples are reported in which such supramolecular assemblies act as hosts for small ions[2] or molecules,[3] large organic compounds[4] or transition-metal complexes.[5] In particular, the ability of supramolecular hosts to act as so-called "molecular flasks" leading to unusual reactivities and selectivities is an interesting advantage,[6] offering new opportunities to steer and control catalytic reactions. In this perspective, catalyst encapsulation is a fascinating method to achieve site-isolation in homogeneous catalysis. Besides control over selectivity, the catalyst is also protected from the bulk, potentially supressing (self-)deactivation. For example, unwanted radical–radical coupling is an important catalyst deactivation pathway[7e] in metallo-radical catalysis[7] that can possibly be prevented by encapsulation of the metallo-radical catalyst in a capsule. Such a site-isolation methodology mimics in a way the protective protein matrix surrounding the active sites of metallo-enzymes, which frequently follow related metallo-radical pathways. Self-deactivation seems to be particularly important in metalloporphyrin-catalysed processes, and hence the development of new hosts that are capable of encapsulating metalloporphyrins is an important goal to advance porphyrin-based (radical-type) catalysis. Only a few papers have so far addressed this problem of self-deactivation in porphyrin-catalysed processes using supramolecular approaches.[8,9]

Due to their symmetry and versatility, porphyrins are widely used for the design of supramolecular host complexes.[10] They are easily accessible and adjustable in terms of substituents and metals, and hence offer various synthetic possibilities and handles to steer the electronic and structural parameters of new (supramolecular) catalysts. Although the encapsulation of porphyrins in so-called metal–organic frameworks (MOFs)[11] is well-established, fewer examples are known in which they are guests in soluble, molecular hosts.[8,9,12] Here we report the synthesis of a new, self-assembled Nitschke-type cubic M_8L_6 cage compound[13] that efficiently encapsulates tetra(4-pyridyl)metalloporphyrins (M(TPyP)). The cage has sufficient space for additional or-

[a] Dr. M. Otte, P. F. Kuijpers, Prof. Dr. J. N. H. Reek, Prof. Dr. B. de Bruin
Homogeneous and Supramolecular Catalysis Group
Van 't Hoff Institute for Molecular Science (HIMS)
University of Amsterdam (UvA), Science Park 904
1098 XH Amsterdam (The Netherlands)
E-mail: b.debruin@uva.nl

[b] Dipl.-Chem. O. Troeppner, Prof. Dr. I. Ivanović-Burmazović
Lehrstuhl für Bioanorganische Chemie
Department Chemie und Pharmazie
Friedrich-Alexander-Universität Erlangen
Egerlandstrase 3, 91058 Erlangen (Germany)

Supporting information for this article is available on the WWW under http://dx.doi.org/10.1002/chem.201301411.

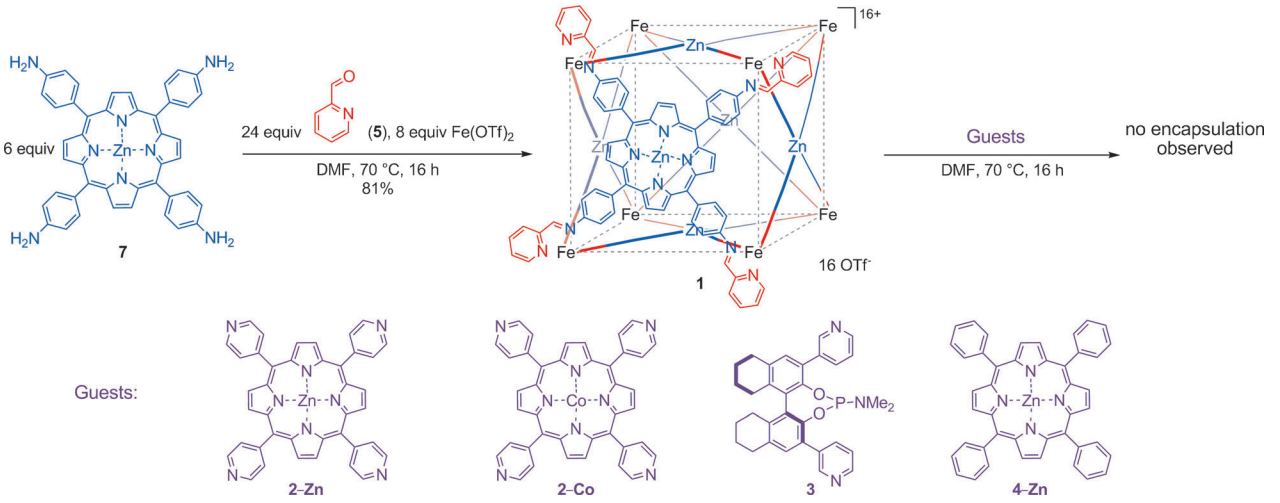

Scheme 1. Synthesis of Nitschke's cubic M_8L_6 cage **1**[13a] and encapsulation studies.

ganic substrates and allows catalytic turnover inside the supramolecular cavity.

Results and Discussion

The deactivation of catalysts via the formation of bridged dimers is an important issue in metalloporphyrin-catalysed processes. Prominent examples are the oxo-bridged dimers in manganese–porphyrin-catalysed epoxidations of olefins, which has been addressed by Hupp and co-workers.[8,9] In our previous studies we reported that dimerisation can also occur in cobalt(II)–porphyrin-catalysed reactions of diazo compounds.[7e] Although this reaction provided additional experimental proof for radical-type pathways in cobalt–porphyrin-catalysed carbene transfer reactions,[7] it also revealed the problem of unwanted catalyst self-deactivation through radical–radical coupling processes in cobalt–porphyrin-catalysed carbene transfer reactions. We took it as a challenge to avoid such self-deactivation processes, and hence we became interested in the use of supramolecular hosts capable of encapsulating porphyrins while leaving enough space available for organic substrates to react inside the cavity. Diamagnetic M_8L_6 cage **1** (Scheme 1) which has been described by Nitschke and co-workers initially looked promising for this purpose.[13a]

The zinc–porphyrin planes of **1** allow, in principle, directed interactions with guests, such as *meso*-tetra(4-pyridyl)porphyrin (H_2-TPyP, **2-H$_2$**), their metalloporphyrin analogues (M^{II}-TPyP, **2-M**) or phosphoramidite ligand **3**, which proved to be valuable in homogeneous catalysis,[14] to give host–guest complexes [**2-H$_2$@1**], [**2-M@1**] or [**3@1**]. Unfortunately, the cubic cage host **1** is not large enough to encapsulate pyridine-appended porphyrins, such as **2-Zn** or **2-Co**. The Zn–Zn distance between two cube planes in **1** is about 15.0 Å, which is smaller than the N–N distance between two *trans*-pyridyl nitrogen atoms in **2** (15.5 Å). Moreover, all attempts to encapsulate porhyrin **4-Zn** and phosphoramidite ligand **3** in **1** were unsuccessful in our hands. We, therefore, decided to design and synthesise a new M_8L_6 cubic cage, which is large enough to host **2**.[15]

Synthesis and characterisation of large cubic M_8L_6 cage 8: We approached the synthesis of a larger cubic cage by replacing the 2-pyridine-aldehyde (**5**) moiety originally used by the 5-bipyridine-aldehyde building block **6** (Scheme 2). Treatment of 24 equiv **6** with 6 equiv of the tetra(4-aminophenyl)porphyrinatozinc(II) building block **7** in the presence of 8 equiv $Fe(OTf)_2$ resulted in the selective formation of the new, larger cubic cage complex **8** through self-as-

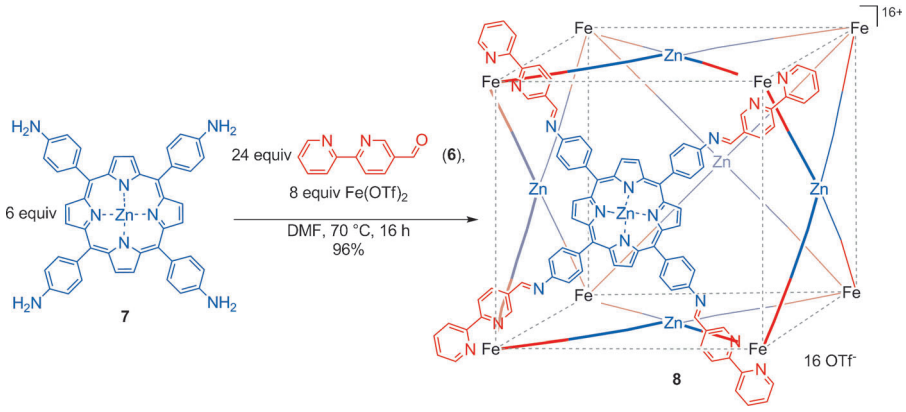

Scheme 2. Synthesis of the new and large cubic M_8L_6 cage **8**.

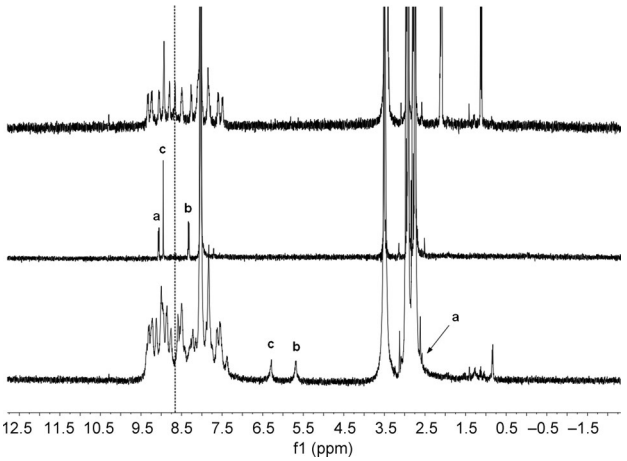

Figure 1. Top: ^{1}H NMR spectrum of **8**. Middle: ^{1}H NMR spectrum of **2-Zn**. Bottom: ^{1}H NMR spectrum of [**2-Zn**@**8**]. All spectra were recorded in [D_7]DMF. Assignment of signals a, b, c follows the labelling of **2-M** shown in Scheme 3.

sembly. Notably, **8** is formed in high yields (96%), and the reaction is relatively easy to scale-up to yield **8** in 400 mg isolated yield. Figure 1 (top) shows the ^{1}H NMR spectrum of cage **8**. Except for one missing signal (belonging to the porphyrin–aniline moiety), the chemical shifts, relative integrals and multiplicity of the signals observed match well with the structure of **8**. Other signals stem from the solvents used (and a minor trace of **6**; signal at 10.3 ppm). Solutions of **8** in DMF are remarkably stable, and remain unchanged for several days at room temperature. To reveal any missing signal hidden under the solvent peaks we performed DOSY experiments (Figure 2). The DOSY separated spectrum clearly revealed that all signals assigned to the cage indeed belong to only one compound. Furthermore, DOSY experiments helped to assign the missing ^{1}H NMR signal of the porphyrin building block hidden under the [D_7]DMF solvent peak at 8.0 ppm, which could not be identified by using

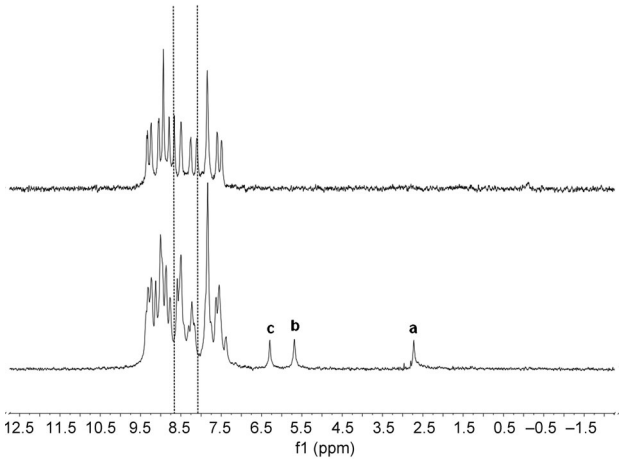

Figure 2. Top: ^{1}H DOSY separated NMR spectrum of **8**. Bottom: ^{1}H DOSY separated NMR spectrum of [**2-Zn**@**8**]. All spectra were recorded in [D_7]DMF. Assignment of signals a, b, c follows the labelling of **2-M** shown in Scheme 3.

^{1}H,^{1}H COSY techniques. ^{13}C NMR spectroscopy data further support the structure of **8** in solution (see the Supporting Information). ^{19}F NMR spectroscopy data showed no indication for encapsulation of the triflate counter ions by **8**. The exact mass of **8** was unambiguously confirmed by Cryo-UHR-ESI-ToF mass spectrometry (see the Supporting Information). Unfortunately, thus far, we have been unable to grow crystals suitable for X-ray diffraction. A MM-minimised model (Spartan'08, SYBYL force field) of **8** is shown in Figure 3. From this model it is clear that cage **8** is larger

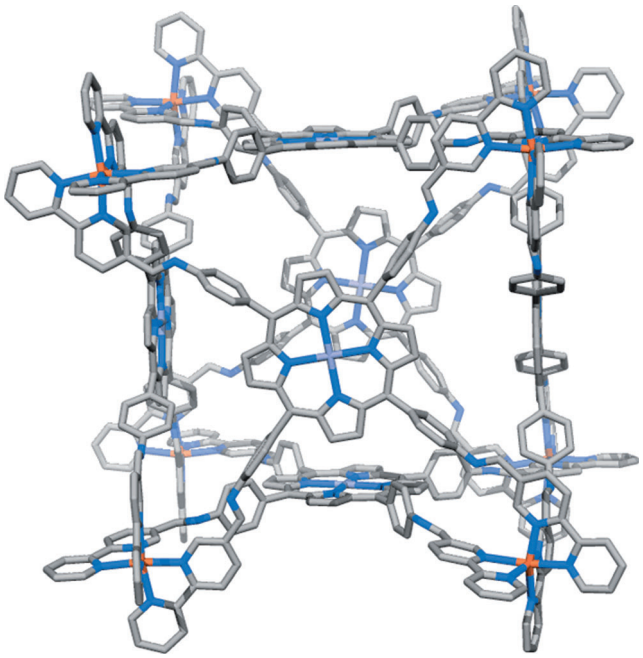

Figure 3. Model (Spartan'08, MM SYBYL FF) of empty cage **8** (hydrogen atoms and counter ions are omitted for clarity).

than cage **1**. The average Zn–Zn distance between two opposite planes in the empty cage **8** (19.5 Å) is about 4.5 Å larger than the corresponding plane distance in **1**. Hence, by modifying the aldehyde building block, derivatives of **1** can be synthesised that offer significantly larger cavities, expanding the scope of host–guest chemistry applications for this new family of M_8L_6 cubic cages.

Encapsulation of metalloporphyrins by cubic host 8: With the new large cubic cage compound **8** in hand we became interested in testing its ability for encapsulating guests (Scheme 3, left). The cavity of **8** is, according to molecular modelling, sufficiently large to host tetra(4-pyridyl)metalloporphyrins (**2**). Indeed, reaction of a 1:1 mixture of **8** and **2-Zn** ([(TPyP)Zn]) gives the new diamagnetic host–guest complex [**2-Zn**@**8**] in 86% yield (Scheme 3). The ^{1}H NMR spectra clearly show the appearance of two new, strongly upfield shifted signals at 6.3 and 5.7 ppm stemming from encapsulated **2-Zn** (Figure 1 bottom; for assignment see Figure 1 and Scheme 3). The observed strong upfield

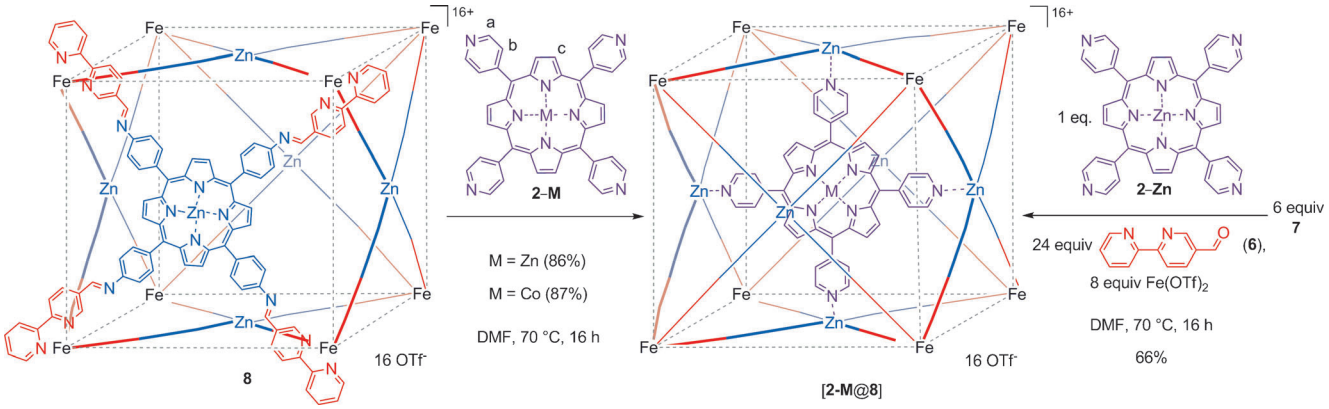

Scheme 3. Left: encapsulation of **2-M** (M = Zn, Co) in **8**. Right: one-step synthesis of [**2-Zn@8**] by using **7** as the substrate.

shifts for **2-Zn** are expected due to anisotropic ring-current effects in the confined nanospace of **8**, and are consistent with data reported in related host–guest assemblies.[12b] The signals of **2-Zn** reveal C_4-symmetry of this encapsulated guest, showing that **2-Zn** is symmetrically bound in **8**. Moreover, as a consequence of the reduced symmetry of host **8** upon binding **2-Zn** (Figure 4), the signals belonging to the

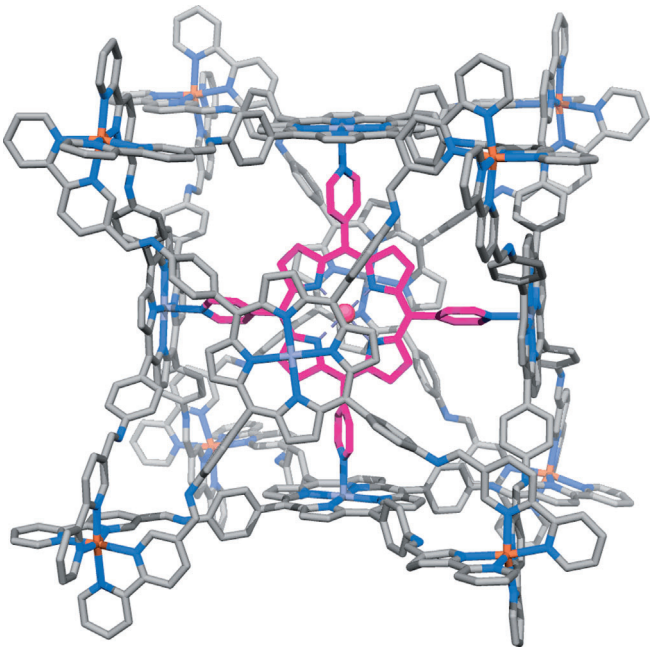

Figure 4. Model (Spartan'08, MM SYBYL FF) of [**2-Co@8**] (hydrogen atoms and counter ions are omitted for clarity).

cage become broader and split-up. The DOSY separated spectrum of [**2-Zn@8**] (Figure 2, bottom) was again required to detect all signals separated from solvent signals, for example, the signal at 2.7 ppm stemming from encapsulated **2-Zn**, and revealed that the assembly [**2-Zn@8**] is indeed one supramolecular molecule in solution. The symmetry, the upfield shifts of all pyridine moieties and the integrals of the ^{1}H NMR signals rule out that guest **2-Zn** binds to host **8** from the outside of the cage. The exact mass of [**2-Zn@8**] was unambiguously confirmed by Cryo-UHR-ESI-ToF mass spectrometry (see the Supporting Information), thus confirming inclusion of exactly one molecule of **2-Zn** in host **8**. No other assemblies with different stoichiometries (e.g., [(**2-Zn**)$_2$**@8**] or [**2-Zn@8**$_2$]) were observed. Moreover, no signals corresponding to empty cage **8** were observed, indicating that no empty host remains after reaction with 1 equiv of porphyrin. The NMR spectra shown in Figures 1 and 2 confirm that no empty cage is left (line as a guide for the eyes).

In a separate experiment we demonstrated that formation of the assembly [**2-Zn@8**] can also be achieved in a one-pot synthetic procedure by mixing **2-Zn**, **6**, **7** and $Fe(OTf)_2$ in the correct stoichiometric amounts (Scheme 3, right). These results underline the highly selective assembly to [**2-Zn@8**] and expanded scope of M_8L_6 cubic cages through selective cavity size variation.

Similar results were obtained when using **8** and the related tetra(4-pyridyl)porphyrinatocobalt(II) (TPyP)Co^{II} (**2-Co**), showing that the approach to encapsulate metalloporphyrins in host **8** is general. The stoichiometry and exact mass of the paramagnetic host–guest assembly [**2-Co@8**] was revealed by Cryo-UHR-ESI-ToF mass spectrometry (Figure S16 in the Supporting Information). Again, no signals corresponding to empty cage **8** were observed. A MM-minimised model of [**2-Co@8**] is shown in Figure 4, illustrating that metalloporphyrins of the type **2-M** fit perfectly in the cavity of the cubic cage **8**.

EPR spectra of [**2-Co@8**] are clearly different from those of free **2-Co**, and illustrate selective encapsulation of **2-Co** in **8** (Figure 5). The EPR spectrum of **2-Co** in frozen DMF reveals a broad, featureless signal. In the region between 5000–1500 gauss only a single broad line was detected (Figure 5, top). Similar signals, albeit much sharper (and therefore revealing resolved cobalt hyperfine couplings), have been reported for $S = {}^1/_2$ (por)Co systems with axially bound pyridine or related σ-donor ligands.[16] Strong dilution of the sample had no effect, and did not lead to sharper or different signal shapes. The spectrum indicates a mixture of self-aggregated assemblies due to intermolecular Co–pyridine interactions between different species **2-Co**. Importantly the EPR spectrum of [**2-Co@8**] is markedly different (Figure 5, bottom). It is much sharper, shows a larger aniso-

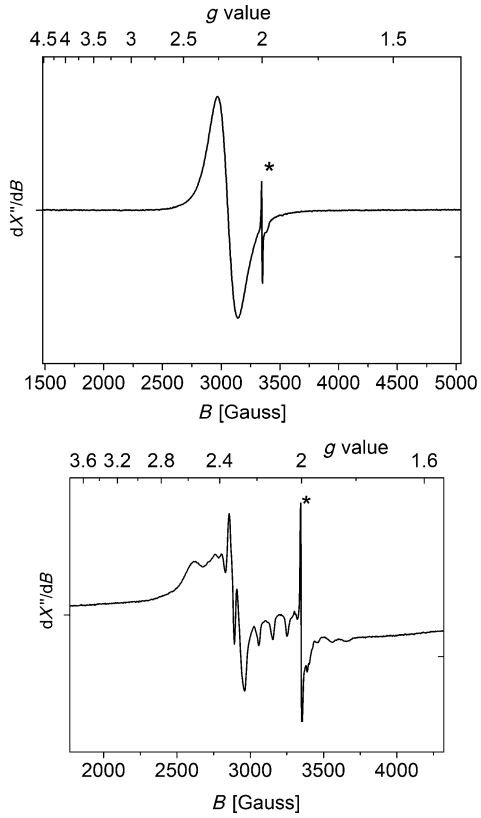

Figure 5. Top: EPR spectrum of **2-Co** recorded in frozen DMF at 20 K. Bottom: EPR spectrum of [**2-Co@8**] recorded in frozen DMF at 20 K. For both spectra the signals marked with and an asterisk are due to an impurity in the EPR cryostat (also detected without a sample tube).

tropy and reveals clearly resolved cobalt hyperfine couplings. The signal is typical for $S=^1/_2$ (por)Co^{II} metallo-radicals with weakly coordinating axial ligands (likely DMF).[17] Clearly, encapsulation of **2-Co** by host **8** protects the system from self-aggregation, and the cubic M_8L_6 host isolates the paramagnetic centres [**2-Co@8**] separated from each other. The diamagnetic free host **8** is EPR silent.

Additional evidence for encapsulation of **2-Co** in **8** was obtained through metallo-radical-trapping experiments. The paramagnetic nature of [**2-Co@8**] prevented us from directly detecting the characteristic NMR signals of encapsulated **2-Co**, and therefore, we decided to convert the metallo-radical [**2-Co^{II}@8**] into a diamagnetic species ([**2-Co^{III}-R@8**]) by treating the Co^{II} centre with ethyl diazoacetate (**9**) in the presence of the hydrogen-atom-transfer (HAT) agent 1,4-cyclohexadiene (**10**; Scheme 4). In this way, diamagnetic [**2-Co^{III}-CH_2CO_2Et@8**] could be obtained. [**2-Co^{III}-CH_2CO_2Et@8**] indeed revealed clear upfield-shifted TPyP signals comparable to those observed for [**2-Zn@8**] (see the Supporting Information). Moreover, the exact mass of [**2-Co^{III}-CH_2CO_2Et@8**] was unambiguously confirmed by Cryo-UHR-ESI-ToF mass spectrometry (see the Supporting Information). This not only proves selective encapsulation of **2-Co** in **8**, but also reveals the accessibility of the catalytically active (TPyP)Co^{II} moiety within the cavity of **8** towards substrates. In agreement, TGA experiments suggest inclusion of a substantial number of solvent molecules in the cavity of [**2-Co@8**] (see the Supporting Information). Notably, we found no indication for the encapsulation of **3** or **4-Zn** in cage **8**. These results underline the selective encapsulation of **2-M** in **8**.

Metallo-radical catalysis: To prove that [**2-Co@8**] is a catalytically active "molecular flask", and the concept that "caging" can have a beneficial influence on the catalytic performance of metallo-radical catalysts, we studied the activity of [**2-Co@8**] in catalysing transformations of diazo compounds. Moreover, we compared the obtained results with several other cobalt(II)–porphyrins, namely (TPP)Co^{II} (**4-Co**), (TPyP)Co^{II} (**2-Co**), (TPyP)Co^{II}*4(TPP)Zn (**2-Co***4(**4-Zn**)) and **11-Co** (Figure 6).[18]

We started our investigations with the cobalt(II)–porphyrin-catalysed radical cyclopropanation of styrene (**12**) with ethyl diazoacetate (**9**) in DMF to give cyclopropane **13** (Table 1).[7,19,20] Indeed, the "caged catalyst" [**2-Co@8**] is

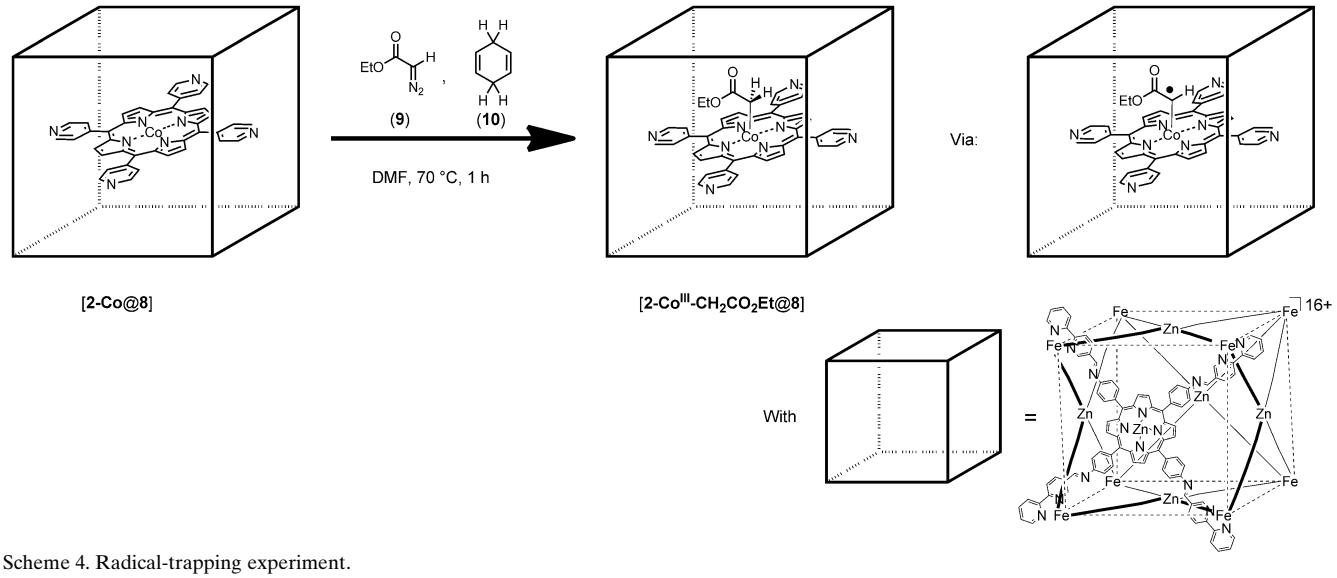

Scheme 4. Radical-trapping experiment.

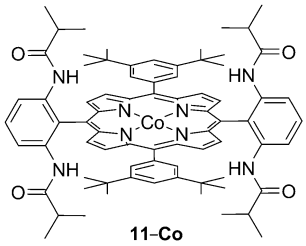

Figure 6. Structure of catalyst **11-Co** reported by Zhang et al.[18]

Table 1. Cobalt-catalysed cyclopropanation of styrene.[a]

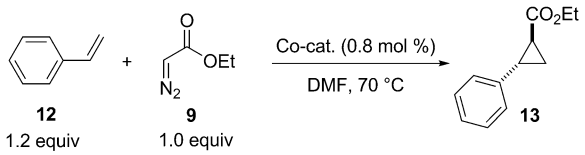

Entry[b]	Catalyst	*t* [h]	Yield [%]	d.r. (*trans*/*cis*)	TON[c]
1	–	1	trace	unknown	–
2	**4-Co**	1	34	78:22	41
3	**2-Co**	**1**	**7**	**67:33**	**9**
4	**2-Co***4(**4-Zn**)	1	10	79:21	13
5	**8**	1	trace	unknown	–
6	[**2-Co@8**]	1	28	65:35	33
7	–	4	trace	unknown	–
8	**4-Co**	4	37	78:22	44
9	**2-Co**	4	15	75:25	18
10	**2-Co***4(**4-Zn**)	4	15	78:22	18
11	**[2-Co@8]**	**4**	**50**	**63:37**	**60**
12	**11-Co**	4	56	74:26	70

[a] The entries in bold highlight the effect of the caged porphyrins. [b] Reaction conditions: **12** (1.16 mmol), **9** (960 μmol), catalyst (8 μmol), DMF (3.2 mL), 70 °C, argon atmosphere. [c] TON (turnover number) = number cycles/number sites within 1 or 4 h.

active in small catalyst loadings (0.8 mol %) towards the formation of **13** (entry 6, 28 %, TON = 33; TON (turnover number) = number cycles/number sites within indicated time).[21] Control experiments show that [**2-Co@8**] is substantially more active than the free tetra(4-pyridyl)porphyrin catalyst **2-Co** (entry 3, 7 %, TON = 9), which is not surprising given the self-aggregation behaviour of **2-Co** (Figure 5). Encapsulation of **2-Co** in **8** protects the cobalt–porphyrin catalyst **2-Co** from deactivating itself via pyridine–cobalt coordination, which blocks its active sites. More noteworthy is the fact that [**2-Co@8**] is almost as equally active as free tetra(phenyl)porphyrin catalyst **4-Co** (compare entries 2 and 6). Hence, **2-Co** must be tightly bound in the protective cage **8** and apparently does not easily escape from the cage, in which case a similar poor activity to that observed for free **2-Co** would be expected (entry 3). Notably, a mixture of **2-Co** with 4 equiv of (TPP)Zn (**4-Zn**) (**2-Co***4(**4-Zn**)) gave very poor results in this reaction (entry 4, 10 %, TON = 13); hardly better than free **2-Co**. The improved activity and enhanced catalytic lifetime of [**2-Co@8**] compared to **2-Co***4(**4-Zn**) can be explained by a stronger binding and better protection of **2-Co** in **8**. Importantly, the empty cage **8** shows no catalytic activity at all, thus ruling out that the iron cage corners are involved in the cyclopropanation reaction (entry 5). To the best of our knowledge, these are the first examples of transition-metal catalysed radical-type reactions of diazo compounds occurring inside the cavity of a supramolecular cage. The M_8L_6 cage **8** has apparently two major effects on the activity of cobalt–porphyrin **2-Co** in [**2-Co@8**]: 1) it activates the encapsulated guest as a catalytically active species, and 2) it (sterically) delays unwanted radical-type side reactions (e.g., radical–radical coupling or catalyst deactivation via HAT). These effects were confirmed by additional experiments described below.

The yield and turnover number achieved with "caged catalyst" [**2-Co@8**] (entry 11, 50 %, TON = 60) after a longer reaction time (4 h) is substantially higher than with the non-protected catalysts **4-Co** (entry 8, 37 %, TON = 44) or **2-Co** (entry 9, 15 %, TON = 18). Also, **2-Co***4(**4-Zn**) gave a lower yield and turnover number (entry 10, 15 %, TON = 18). Moreover, the turnover numbers of **4-Co** do not differ significantly between 1 and 4 h reaction time, indicating that **4-Co** became inactive after 1 h of reaction (entries 2 and 8), whereas the encapsulated catalyst [**2-Co@8**] remained active in this period (entries 6 and 11) effectively leading to higher yields (50 %) than obtained with **4-Co** (37 %) after 4 h in DMF.[21] From all tested catalysts, **11-Co** is the only one that overall performs better than [**2-Co@8**] (entry 12, 56 %, TON = 70) under the applied reaction conditions. In a way, the steric bulk of this catalyst likely provides a similar protective "cage" around the metal as is the case for [**2-Co@8**], but additionally the H-bonding motifs contribute to the relatively high activity of **11-Co**.[7a]

To further explore the scope of [**2-Co@8**] towards diazo compounds capable of entering the cage and reacting with the encapsulated cobalt centre, we tested the reactivity of diazo ester **14** (Scheme 5). Activation of **14** with cobalt(II)–porphyrins yields carbon centred radical **15**. In the absence of any external radical acceptor, intermediate **15** can in principle undergo two different reaction pathways. Intramolecular radical addition to the aromatic ring results in the forma-

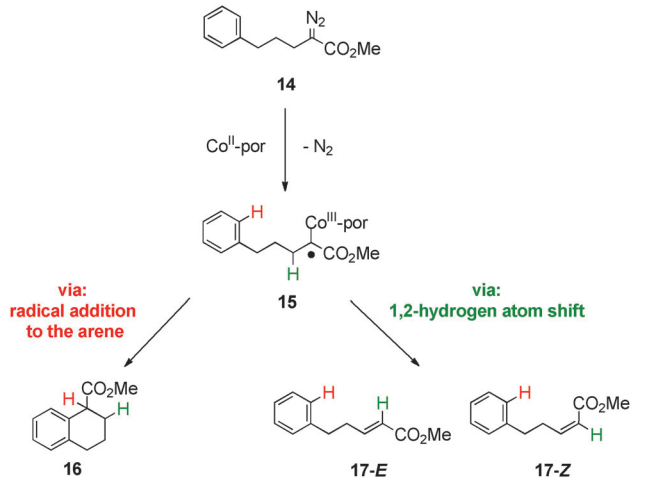

Scheme 5. Intramolecular reactions of **15**.

tion of **16**, similar to the approach described by Gansäuer, Flowers and co-workers.[22] Alternatively, a 1,2-hydrogen atom shift yields the olefins **17**. Although olefin formation from diazo compounds has been described for other catalysts based on rhodium or copper,[23] cobalt(II)–porphyrin-catalysed olefin formation from diazo esters like **14** has not been described to date.

Table 2 gives an overview of the results obtained when treating **14** with 1 mol% of the cobalt catalysts mentioned above. In none of the performed experiments cyclisation product **16** could be observed. Employing (TPP)Co^{II} (**4-Co**) as a catalyst yields **17** as sole product after 1 h, but in poor yield and with poor diastereoselectivity (entry 1, 10%, E/Z = 40:60, TON = 10). Free **2-Co** gave **17** only in trace amounts (entry 2). Notably, the encapsulated catalyst [**2-Co@8**] gave the best results after 1 h in terms of yield (30%) and diastereoselectivity favouring **17-*Z*** over **17-*E*** (entry 3, E/Z = 13:87). Increasing the reaction time to 3 h further improved the yield (entry 4, 40%, E/Z = 14:86). Remarkably, whereas **11-Co** gave better results in the cyclopropanation of styrene than [**2-Co@8**], the situation was clearly reversed for the transformation of **14** to **17**. Catalyst **11-Co** produced olefin **17** with a significant lower yield but slightly higher diastereoselectivity (entry 5, 20%, E/Z = 10:90) than [**2-Co@8**] (entry 4, 40%, E/Z = 16:84). Increasing the loading of employed catalyst further improved the yield. Catalyst [**2-Co@8**] clearly gave the best results with 72% yield (entry 9, 72%, E/Z = 16:84). The mixture of **2-Co** with 4 equiv of (TPP)Zn (**4-Zn**) (**2-Co***4(**4-Zn**)) gave only 15% of **17** in 3 h under similar reaction conditions (entry 8). These results undoubtedly demonstrate that the reactivity of a cobalt–porphyrin can be dramatically influenced by encapsulation in a supramolecular host.

Table 2. Cobalt-catalysed synthesis of olefins **17**.[a]

Entry[b]	Catalyst	mol%	*t* [h]	Yield **17** [%]	d.r. (*E*/*Z*)
1	**4-Co**	1	1	10	40:60
2	**2-Co**	1	1	trace	unknown
3	**[2-Co@8]**	**1**	**1**	**30**	**13:87**
4	**[2-Co@8]**	**1**	**3**	**40**	**16:84**
5	**11-Co**	1	3	20	10:90
6	**4-Co**	2	3	22	43:57
7	**2-Co**	2	3	<7	22:78
8	**2-Co***4(**4-Zn**)	2	3	15	29:71
9	**[2-Co@8]**	**2**	**3**	**72**	**16:84**

[a] The entries in bold highlight the effect of the caged porphyrins. [b] Reaction conditions: **14** (0.5 mmol), DMF (2.5 mL), 70°C, argon atmosphere.

Conclusion

We here present the design, synthesis and characterisation of a new "molecular flask". This M_8L_6 cubic cage is sufficiently large to encapsulate tetra(4-pyridyl)porphyrins, which represent an important class of catalysts. The synthesis of this host is based on a self-assembly process using Bipy-functionalised porphyrin building blocks. The encapsulation of tetra(4-pyridyl)metalloporphyrins, as presented here, provide the first examples of encapsulated transition-metal complexes in such hosts. Importantly, the encapsulated porphyrins are active catalysts and show higher TON than the non-encapsulated analogues in radical-type transformations as the shielded environment reduces the number of unwanted side reactions of reactive radical intermediates. The systems presented here are rare examples of (molecularly) caged metalloporphyrins capable of catalytic turnover. The encapsulated tetra(4-pyridyl)porphyrinatocobalt(II) (TPyP)Co (**2-Co**) was active in radical-type cyclopropanation of styrene with ethyl diazoacetate as well as *Z*-selective olefin synthesis using a disubstituted diazo compound as the substrate. Improved activities and catalyst lifetimes were demonstrated through a combination of control experiments. The results show that the reactivity of a transition-metal complex can be dramatically influenced by encapsulation in a supramolecular host.

We are currently exploring the full potential of this system in (metalloradical-type) reactions. Moreover, we aim at the synthesis of new, neutral and robust hosts (e.g., those lacking imine functionalities) to further expand the scope and usability of this new class of supramolecular hosts.

Experimental Section

Synthesis of 6: $Pd(PPh_3)_2Cl_2$ (104 mg, 0.15 mmol), PPh_3 (77 mg, 0.30 mmol), 2-(tributylstannyl)pyridine (1.09 g, 2.95 mmol), 6-bromo-3-pyridinecarbaldehyde (660 mg, 3.54 mmol) and toluene (40 mL) were added to an oven-dried Schlenk flask under argon. The resulting mixture was stirred for 72 h under reflux. The resulting mixture was cooled to room temperature and the solvent was removed under reduced pressure. The obtained solid was dissolved in CH_2Cl_2 (50 mL) and washed with a saturated NH_4Cl solution (30 mL). The aqueous phase was extracted with CH_2Cl_2. The organic layers were combined, the solvent was removed under reduced pressure and the crude product was purified by SiO_2 chromatography (20% EA, 20% CH_2Cl_2 and 60% CH, R_f = 0.16) to give **6** (200 mg, 1.09 mmol, 37%) as a colourless solid. ^{1}H NMR (300 MHz, $CDCl_3$): δ = 10.18 (s, 1H), 9.13 (d, J = 2.1 Hz, 1H), 8.76–8.71 (m, 1H), 8.63 (d, J = 8.5 Hz, 1H), 8.52 (m, 1H), 8.30 (dd, J = 8.2 Hz, J = 2.1 Hz, 1H), 7.89 (td, J = 7.8 Hz, J = 1.9 Hz, 1H), 7.40 ppm (ddd, J = 7.5 Hz, J = 4.8 Hz, J = 1.2 Hz, 1H); ^{13}C NMR (75 MHz, $CDCl_3$): δ = 190.8, 160.7, 154.8, 151.8, 149.6, 127.4, 137.1, 131.2, 125.0, 122.4, 121.5 ppm; ^{1}H and ^{13}C NMR data are in agreement with those published.[24]

Synthesis of 8: Compound **7** (48.8 mg, 66 μmol), $Fe(OTf)_2$ (30.5 mg, 88 μmol), **6** (48.6 mg, 264 μmol) and DMF (5 mL) were mixed in an oven-dried Schlenk flask under an argon atmosphere. The mixture was degassed three times and stirred for 16 h at 70°C. The mixture was cooled to room temperature and diethyl ether was added. The mixture was filtered and washed with diethyl ether. The remaining solid was dissolved in DMF. The solvent was removed under reduced pressure to give **8** as a purple solid (119 mg, 10.6 μmol, 96%). ^{1}H NMR (400 MHz, [D_7]DMF): δ = 9.33 (d, J = 9.3 Hz, 24H, H-5), 9.24 (d, J = 8.4 Hz, 24H, H-4), 9.05 (d, J = 8.2 Hz, 24H, H-6), 8.93 (s, 48H, H-11), 8.79 (s, 24H, H-8), 8.66 (s, 24H, H-7), 8.45 (s, 24H, H-3), 8.25 (d, J = 8.6 Hz, 24H, H-10), 8.10 (m, 24H, H-10′), 7.87–7.79 (m, 48H, H-1, H-2), 7.60 (d, J = 8.4 Hz, 24H, H-9), 7.48 ppm (d, J = 8.5 Hz, 24H, H-10′); ^{13}C NMR (125 MHz, [D_7]DMF): δ = 160.50, 159.58, 158.41, 156.01, 152.84, 152.33, 151.00, 150.83, 142.39, 140.50, 137.37, 137.17, 136.96, 136.65, 132.78, 132.46, 129.60, 126.68, 125.87, 124.10, 121.52, 121.39, 118.70 ppm; ^{19}F NMR (282 MHz, [D_7]DMF): δ = −77.5 ppm; IR (neat): $\tilde{\nu}$ = 2970, 2360, 2340,

1660, 1390, 1255 1155, 1090, 1030 cm^{-1}; UV/Vis (DMF): λ_{max} = 312, 359, 424, 443, 565, 607 nm; exact mass ESI-MS: see Table S1 in Supporting Information.

Synthesis of [2-Zn@8]: *Encapsulation of **2-Zn** in preformed cubic cage **8***: compound **8** (150 mg, 134 μmol), **2-Zn** (9.1 mg, 134 μmol) and DMF (20 mL) were treated in the same manner as for the synthesis of **8** to give **[2-Zn@8]** as a purple solid (137 mg, 11.4 μmol, 85%).

*One-step synthesis of **[2-Zn@8]** starting from **7***: Compound **7** (30 mg, 41 μmol), $Fe(OTf)_2$ (19 mg, 53 μmol), **6** (30 mg, 164 μmol), **2-Zn** (4.2 mg, 6.8 μmol) and DMF (5.0 mL) were treated in the same manner as for the synthesis of **8** to give **[2-Zn@8]** as a purple solid (53 mg, 4.4 μmol, 65%). ^{1}H NMR (400 MHz, [D_7]DMF): δ = 9.46–9.19 (m, 44H), 9.18–8.69 (m, 102H), 8.68–8.06 (m, 90H), 8.01–7.72 (m, 55H), 7.71–7.34 (m, 45H), 6.3 (s, 8H), 5.77–5.65 (m, 8H), 2.81–2.67 ppm (m, 8H); ^{13}C NMR (125 MHz, [D_7]DMF): δ = 160.45, 160.00–159.30, 158.71–158.03, 155.88, 152.81, 151.45–151.01, 150.73, 149.19, 147.75, 142.47–141.74, 140.33, 137.87–136.16, 133.09–132.00, 130.51, 129.50, 126.52, 125.71, 123.87, 121.67–120.71, 119.37–118.14, 116.52, 113.60 ppm; IR (neat): $\tilde{\nu}$ = 2360, 2340, 2260, 1650, 1255, 1155, 1030, 660, 635, 460 cm^{-1}; UV/Vis (DMF): λ_{max} = 315, 356, 413, 450, 567, 611 nm; exact mass ESI-MS: see Table S3 in the Supporting Information.

Synthesis of [2-Co@8]: Compound **2-Co** (7.4 mg, 11 μmol), **8** (125 mg, 11 μmol) and DMF (10 mL) were treated in the same manner as for the synthesis of **8** to give **[2-Co@8]** as a purple solid (114.5 mg, 9.6 μmol, 87%). ^{19}F NMR (282 MHz, [D_7]DMF): δ = −77.5 ppm; IR (neat): $\tilde{\nu}$2365, 2340, 1655, 1250, 1225, 1150, 1030, 990, 790, 635, 635, 435, 410 cm^{-1}; UV/Vis (DMF): λ_{max} = 316, 357, 420, 443, 567, 610 nm; exact mass ESI-MS: see Table S4 in the Supporting Information; for TG/DSC see Figure S16 in the Supporting Information.

Synthesis of [2-Co^{III}-CH_2CO_2Et@8]: Compound [**2-Co@8**] (32 mg, 2.7 μmol) and DMF (0.5 mL) were added to an oven-dried Schlenk flask under nitrogen. Ethyl diazoacetate (70 mg, **12**, 620 μmol) and 1,4-cyclohexadiene (9 mg, **13**, 110 μmol) were added to the stirred solution and the mixture was heated to 70°C. After 90 min the solution was cooled to room temperature and dry diethyl ether (10 mL) was added. The obtained suspension was filtered and the remaining solid was washed with diethyl ether. After being dried under reduced pressure [**2-Co^{III}-CH_2CO_2Et@8**] was obtained as a dark purple solid (17 mg). ^{1}H NMR (400 MHz, [D_7]DMF): δ = 9.45–8.69 (m, 155H), 8.69–8.13 (m, 72H), 8.13–7.89 (m, 44H), 7.89–7.07 (m, 65H), 6.50–6.31 (m, 8H), 5.84–5.68 (m, 8H), 2.96–2.82 ppm (m, 8H); exact mass ESI-MS: see Table S5 in the Supporting Information.

Synthesis of 2-Co*4(4-Zn): Compound **2-Co** (49.8 mg, 73.7 mmol), **4-Zn** (200 mg, 295 mmol) and DMF (10 mL) were added to an oven-dried Schlenk flask under nitrogen. The stirred reaction mixture was degassed three times and heated to 70°C for 16 h. After the reaction mixture was cooled to room temperature all solvents were removed under vacuum to yield 249 mg of a purple powder.

Generalised procedure for the catalytic cyclopropanation experiments: The cobalt catalyst (8 μmol) and DMF (3.2 mL) were added to an oven-dried Schlenk flask under argon. Compounds **12** (120 mg, 1.16 mmol) and **9** (109 mg, 960 μmol) were added to the mixture and the reaction mixture was stirred for one or four hours at 70°C oil-bath temperature. The mixture was cooled to room temperature and EtOAc was added. After being filtered and washed with EtOAc the solvents were removed from the mixture under reduced pressure and the crude product was purified by SiO_2 chromatography (25% EA, 75% CH) to give **13** as a pale yellow oil. ^{1}H NMR data of thus obtained cyclopropane **13** were in agreement with those published.[20]

Generalised procedure for the synthesis of 17: The cobalt catalyst (10 μmol) and DMF (2.5 mL) were added to an oven-dried Schlenk flask under argon. Compound **14** (109 mg, 500 μmol) was added and the reaction mixture was stirred for the indicated time at 70°C oil-bath temperature. The mixture was cooled to room temperature and EtOAc was added. After filtration and washing with EtOAc the solvents were removed under reduced pressure and mixtures of product **17** and substrate **14** were obtained. ^{1}H NMR data of thus obtained olefins **17** are in agreement with those published.[25]

Acknowledgements

Financial support from the Netherlands Organisation for Scientific Research (NWO-CW VICI project 016.122.613), the European Research Council (ERC, grant agreement 202886-CatCIR), and the University of Amsterdam is acknowledged. M.O. gratefully acknowledges the AvH-Foundation for a Feodor Lynen postdoctoral fellowship. I.I.-B. and O.T. gratefully acknowledge support through the "Solar Technologies Go Hybrid" initiative of the State of Bavaria.

[1] R. Chakrabarty, P. S. Mukherjee, P. J. Stang, *Chem. Rev.* **2011**, *111*, 6810–6918.

[2] a) M. Ziegler, J. L. Brumaghim, K. N. Raymond, *Angew. Chem.* **2000**, *112*, 4285–4287; *Angew. Chem. Int. Ed.* **2000**, *39*, 4119–4121; b) G. Mezei, P. Baran, R. G. Raptis, *Angew. Chem.* **2004**, *116*, 584–587; *Angew. Chem. Int. Ed.* **2004**, *43*, 574–577.

[3] a) N. Branda, R. Wyler, J. Rebek, *Science* **1994**, *263*, 1267–1268; b) P. Mal, B. Breiner, K. Rissanen, J. R. Nitschke, *Science* **2009**, *324*, 1697–1699.

[4] J. C. Chapin, M. Kvasnica, B. W. Purse, *J. Am. Chem. Soc.* **2012**, *134*, 15000–15009.

[5] D. H. Leung, D. Fiedler, R. H. Bergman, K. N. Raymond, *Angew. Chem.* **2004**, *116*, 981–984; *Angew. Chem. Int. Ed.* **2004**, *43*, 963–966.

[6] Examples of "molecular flasks": a) M. Yoshizawa, M. Tamura, M. Fujita, *Science* **2006**, *312*, 251–254; b) T. Yamaguchi, M. Fujita, *Angew. Chem.* **2008**, *120*, 2097–2099; *Angew. Chem. Int. Ed.* **2008**, *47*, 2067–2069; c) M. Yoshizawa, J. K. Klosterman, M. Fujita, *Angew. Chem.* **2009**, *121*, 3470–3490; *Angew. Chem. Int. Ed.* **2009**, *48*, 3418–3438; d) C. J. Brown, R. G. Bergman, K. N. Raymond, *J. Am. Chem. Soc.* **2009**, *131*, 17530–17531; e) Z. J. Wang, C. J. Brown, R. G. Bergman, K. N. Raymond, F. D. Toste, *J. Am. Chem. Soc.* **2011**, *133*, 7358–7360.

[7] a) W. I. Dzik, X. Xu, X. P. Zhang, J. N. H. Reek, B. de Bruin, *J. Am. Chem. Soc.* **2010**, *132*, 10891–10902; b) W. I. Dzik, X. P. Zhang, B. de Bruin, *Inorg. Chem.* **2011**, *50*, 9896–9903; c) A. I. Olivos Suarez, H. Jiang, X. P. Zhang, B. de Bruin, *Dalton Trans.* **2011**, *40*, 5697–5705; d) V. Lyaskovskyy, A. I. Olivos Suárez, H. Lu, H. Jiang, X. P. Zhang, B. de Bruin, *J. Am. Chem. Soc.* **2011**, *133*, 12264–12273; e) H. Lu, W. I. Dzik, X. Xu, L. Wojtas, B. de Bruin, X. P. Zhang, *J. Am. Chem. Soc.* **2011**, *133*, 8518–8521; f) V. Lyaskovskyy, B. de Bruin, *ACS Catal.* **2012**, *2*, 270–279.

[8] M. L. Merlau, W. J. Grande, S. T. Nguyen, J. T. Hupp, *J. Mol. Catal. A* **2000**, *156*, 79–84.

[9] a) M. L. Merlau, M. del Pilar Mejia, S. T. Nguyen, J. T. Hupp, *Angew. Chem.* **2001**, *113*, 4369–4372; *Angew. Chem. Int. Ed.* **2001**, *40*, 4239–4242; b) S. J. Lee, S.-H. Cho, K. L. Mulfort, D. M. Tiede, J. T. Hupp, S. T. Nguyen, *J. Am. Chem. Soc.* **2008**, *130*, 16828–16829.

[10] a) V. F. Slagt, J. N. H. Reek, P. C. J. Kamer, P. W. N. M. van Leeuwen, *Angew. Chem.* **2001**, *113*, 4401–4404; *Angew. Chem. Int. Ed.* **2001**, *40*, 4271–4274; b) M. Kuil, T. Soltner, P. W. N. M. van Leeuwen, J. N. H. Reek, *J. Am. Chem. Soc.* **2006**, *128*, 11344–11345; c) A. K. Bar, R. Chakrabarty, G. Mostafa, P. S. Mukherjee, *Angew. Chem.* **2008**, *120*, 8583–8587; *Angew. Chem. Int. Ed.* **2008**, *47*, 8455–8459; d) I. Beletskaya, V. S. Tyurin, A. Y. Tsivadze, R. Guilard, C. Stern, *Chem. Rev.* **2009**, *109*, 1659–1713.

[11] For examples, see: a) M. H. Alkordi, Y. Liu, R. W. Larsen, J. F. Eubank, M. Eddaoudi, *J. Am. Chem. Soc.* **2008**, *130*, 12639–12641; b) Z. Zhang, W.-Y. Gao, L. Wojtas, S. Ma, M. Eddaoudi, M. J. Zaworotko, *Angew. Chem.* **2012**, *124*, 9464–9468; *Angew. Chem. Int. Ed.* **2012**, *51*, 9330–9334.

[12] a) D. L. Dick, T. V. S. Rao, D. Sukumaran, D. S. Lawrence, *J. Am. Chem. Soc.* **1992**, *114*, 2264–2669; b) S. Anderson, H. L. Anderson, A. Bashall, M. McPartlin, J. K. M. Sanders, *Angew. Chem.* **1995**, *107*, 1196–1200; *Angew. Chem. Int. Ed. Engl.* **1995**, *34*, 1096–1099; c) K. Ono, M. Yoshizawa, T. Kato, K. Watanabe, M. Fujita, *Angew. Chem.* **2007**, *119*, 1835–1838; *Angew. Chem. Int. Ed.* **2007**, *46*, 1803–1806.

[13] Examples of cubic cage compounds described by Nitschke and coworkers: a) W. Meng, B. Breiner, K. Rissanen, J. D. Thoburn, J. K. Clegg, J. R. Nitschke, *Angew. Chem.* **2011**, *123*, 3541–3545; *Angew. Chem. Int. Ed.* **2011**, *50*, 3479–3483; b) M. M. J. Smulders, A. Jiménez, J. R. Nitschke, *Angew. Chem.* **2012**, *124*, 6785–6789; *Angew. Chem. Int. Ed.* **2012**, *51*, 6681–6685; c) C. Browne, S. Brenet, J. K. Clegg, J. R. Nitschke, *Angew. Chem.* **2013**, *125*, 1998–2002; *Angew. Chem. Int. Ed.* **2013**, *51*, 1944–1948.

[14] T. Gadzikwa, R. Bellini, H. L. Dekker, J. N. H. Reek, *J. Am. Chem. Soc.* **2012**, *134*, 2860–2863.

[15] In principle, the synthesis of cubic M_8L_6 cages offering an increased cavity size can be accomplished by changing either one of the three building blocks (tetra-*para*-aniline-zinc-porphyrin (**8**), 2-pyridine-aldehyde (**9**) or $Fe(OTf)_2$) of **5**. The influence of the employed metal salts on size of related tetrahedral M_4L_6 cages has been described very recently: T. K. Ronson, C. Giri, N. K. Beyeh, A. Minkkinen, F. Topić, J. J. Holstein, K. Rissanen, J. R. Nitschke, *Chem. Eur. J.* **2013**, *19*, 3374–3382.

[16] a) F. A. Walker, *J. Am. Chem. Soc.* **1970**, *92*, 4235–4244; b) B. B. Wayland, J. V. Minkiewicz, M. E. Abd-Elmageed, *J. Am. Chem. Soc.* **1974**, *96*, 2795–2801; c) G. P. Däges, J. J. Hütterman, *J. Phys. Chem.* **1992**, *96*, 4787–4794.

[17] a) L. Ukrainczyk, M. Chibwe, T. J. Pinnavaia, S. A. Boydt, *J. Phys. Chem.* **1994**, *98*, 2668–2676; b) D. F. Evans, D. Wood, *J. Chem. Soc. Dalton Trans.* **1987**, 3099–3101.

[18] X. Cui, X. Xu, L. Wojtas, M. M. Kim, X. P. Zhang, *J. Am. Chem. Soc.* **2012**, *134*, 19981–19984.

[19] In coordinating solvents, such as DMF, cyclopropanation reactions are generally associated with lower rates and shorter catalyst lifetimes. This makes it easier to investigate the effect of catalyst "caging" effects in terms of catalyst activity and stability.

[20] L. Huang, Y. Chen, G.-Y. Gao, X. P. Zhang, *J. Org. Chem.* **2003**, *68*, 8179–8184.

[21] For the definition of TON see also: S. Kozuch, J. M. L. Martin, *ACS Catal.* **2012**, *2*, 2787–2794.

[22] A. Gansäuer, M. Behlendorf, D. von Laufenberg, A. Fleckhaus, C. Kube, D. V. Sadasivam, R. A. Flowers II, *Angew. Chem.* **2012**, *124*, 4819–4823; *Angew. Chem. Int. Ed.* **2012**, *51*, 4739–4742.

[23] For an example, see: J. D. Dudones, P. Sampson, *Tetrahedron* **2000**, *56*, 9555–9567.

[24] B. Brisig, E. C. Constable, C. E. Housecroft, *New J. Chem.* **2007**, *31*, 1437–1447.

[25] For **17-*E***, see: A. A. Poeylaut-Palena, S. A. Testero, E. G. Mata, *J. Org. Chem.* **2008**, *73*, 2024–2027; for **17-Z** see: Y.-S. Hon, C.-F. Lee, *Tetrahedron* **2000**, *56*, 7893–7902.

Received: April 14, 2013
Published online: July 2, 2013

